14 Surface Physics

T. Greber, M. Hengsberger, J. H. Dil, F. Matsui, H. Ma, R. Westerström, L. Castiglioni, H. Cun, D. Leuenberger, B. Slomski, S. Roth, A. Hemmi, G. Landolt, M. Greif, C. Janssen, P. Donà, S. Muff, R. Stania, C. Bernard, E. Eisenring, T. Kälin, J. Osterwalder

The group investigates surface and interface phenomena at the atomic level. For this purpose the surface physics laboratory is well equipped for the preparation and characterization of clean single-crystalline surfaces, metal and molecular monolayer films, as well as covalently bonded single layers, using a wide variety of experimental techniques. Moreover, we currently operate two photoemission spectrometers at the nearby Swiss Light Source (SLS), one for spin- and angle-resolved photoemission spectroscopy (SARPES) and one for photoelectron diffraction and holography. Moreover, the group is participating actively in the buildup of the new SLS beamline PEARL (PhotoEmission and Atomic Resolution Laboratory).

The research carried out during the report period can be grouped into four topics:

- **Monolayer films of hexagonal boron nitride (*h*-BN) and graphene on metal surfaces**
  Over the last several years the group has built up a considerable expertise in the growth and characterization of sp^2-bonded monolayers on transition metal surfaces. The current studies are motivated by two different guiding principles. The first one is related to the chemical functionality of the adlayers: on Rh(111) and Ru(0001) surfaces, the large lattice misfit induces strongly corrugated sp^2 layers that exhibit also a corrugation in the electrostatic potential landscape that can be exploited for templating molecular adsorbates [1–4]. We have come to a rather complete understanding of the structure of these layers (see Section 14.1). These layers are very inert and can be brought in contact with air, water and many organic solvents, and they are thus amenable to ex-situ experiments. Within a Sinergia project of the Swiss National Science Foundation, funding a consortium of four different groups, we have built up a growth chamber for handling wafer-size samples, where h-BN or graphene films can be grown on four-inch Si(111) wafers covered with monocrystalline Rh(111) films. The chamber is placed in a dedicated clean-room, which enables us to process these samples in a dust-free environment. First experiments involve the manipulation of the surface energy of such films by hydrogen intercalation, monitored by contact angle measurements, and the preparation of organic light-emitting diodes (OLEDs) where the electrons are injected via a well defined h/BN/Rh(111) interface.

  The second line of research is directed towards the synthesis of epitaxial layers of graphene and h-BN with a view on future electronic devices based on graphene. Due to its insulating properties and similar crystal structure and lattice constant, h-BN appears to be the ideal 'gate oxide'. We have had first successes in growing graphene layers on top of single-layer h-BN on Cu(111) and determining the resulting registry of the two sp^2 lattices. Moreover, based on the progress in the wafer-scale growth of sp^2 layers, making large amounts of samples available, we are currently working on peel-off methods for producing freestanding monolayer films on the centimeter scale.

- **Molecular adsorbates and molecular monolayers**
  The focus on endofullerenes was continued in our endeavour to study monolayer films of magnetic molecules. In a project 'Resonant X-ray Photoelectron Diffraction (RXPD)' funded by the SNF, films of $DySc_2@C_{80}$ molecules, obtained from L. Dunsch of the IWF Dresden, were prepared from minute quantities. They were characterized for their magnetic properties by x-ray magnetic circular dichroism and SQUID (group of H. Keller), and the sam-

ples show long spin relaxation times at a temperature of 2K. The future PEARL beamline at the SLS will permit us to study these molecules in monolayers, using RXPD for combined structural information with sensitivity to magnetism. A first proof-of-principle experiment based on a clean Ni(111) crystal has been published last year [5].

- **Spin-resolved photoemission and momentum mapping**
  Our spin-resolved photoemission chamber (COPHEE) at the SLS has continued to be in high demand as a general user instrument due to its unique performance. In collaboration with several other groups, the ternary compound $PbBi_4Te_7$, a three-dimensional topological insulator, was characterized in terms of its electronic and spin structure [6]. Moreover, the studies of the Rashba effect in ultrathin Pb films on Si(111) were continued (see Sec. 14.2). Further studies included the compound BiTeI, which exhibits a giant Rashba effect in the bulk band structure due to its non-centrosymmetric structure [7], and a homologous series of topological insulators of the composition $GeBi_{4-x}Sb_xTe_7$ (in collaboration with the group of A. Schilling).

- **Ultrafast processes at surfaces**
  Within the NCCR 'Molecular Ultrafast Science and Technology' (MUST), our group has built and commissioned a compact angle-resolved photoemission chamber, which will be moved to various ultrashort pulsed light sources available within the consortium. It is currently stationed at ETH (laboratory of U. Keller), being readied for first attosecond photoemission experiments on self-assembled diamondoid monolayers, which show negative electron affinity. Earlier experiments in our group had provided some clues on the mechanism leading to efficient, largely monochromatic electron emission [8]. Last years activities included a pump-probe time-resolved photoemission study of the Bi(114) surface, where the coherent excitation of a surface-related phonon mode is clearly observed (see Sec. 14.3).

[1] S. Berner *et al.*, Angew. Chem. Int. Ed. 46, 5115 (2007).
[2] J. H. Dil *et al.*, Science 319, 1824 (2008).
[3] T. Brugger *et al.*, Phys. Rev. B 79, 045407 (2009).
[4] A. J. Pollard *et al.*, Angew. Chem. Int. Ed. 49, 1794 (2010).
[5] M. Morscher *et al.*, Phys. Rev. B 84, 140406 (2011).
[6] S. V. Eremeev *et al.*, Nature Commun. 3, 635 (2012).
[7] K. Ishizaka *et al.*, Nature Mat. 10, 521 (2011).
[8] S. Roth *et al.*, Chem. Phys. Lett. 495, 102 (2010).

In the following, three highlights of last year's research are presented in more detail.

14.1 The unit cell of graphene on ruthenium

In collaboration with: Marcella Iannuzzi, Jürg Hutter, Physikalisch Chemisches Institut, Universität Zürich; Irakli Kalichava, Steven J. Leake, Oliver Bunk, Phil Willmott, Swiss Light Source, Paul Scherrer Institut, 5232 Villigen; Haitao Zhou, Geng Li, Yi Zhang, and Hongjun Gao, Institute of Physics, Chinese Academy of Sciences, Beijing, 100190, China.

A single layer of sp^2 hybridized carbon on the (0001) surface ruthenium (g/Ru) forms a corrugated superstructure (see Fig. 14.1) that is related to the mismatch of the two lattice constants. The unit cell corresponds to a coincidence lattice of 25×25 graphene units (1250 atoms) on top of 23×23 ruthenium unit cells and comprises *four* protrusions [1]. These hills are surrounded by *lateral* electric fields that are imposed by the corrugation of the graphene layer [2]. These fields are important for the templating functionality for adsorbed molecules [3], and for understanding scanning tunneling spectroscopy data measured on the hills in terms of local resonances, implying the scenario of graphene based quantum dot arrays [4].

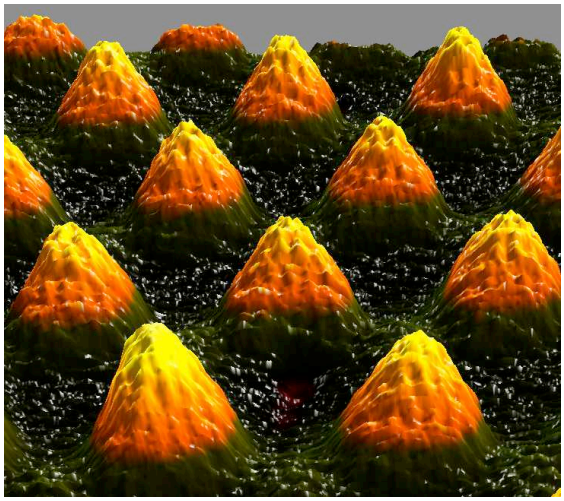

FIG. 14.1 – *Three-dimensional representation of low-temperature scanning tunneling microscopy data of the g/Ru superstructure with atomic resolution. The height of the hills is 0.12 nm, their distance is about 3 nm. The corrugation is of crucial importance for the understanding of this structure and its functionality. Data from H.G. Zhang, cover of J. Phys: Condens Matter 22 No. 30 (2010).*

An earlier surface x-ray diffraction study had concluded that the four hills in the unit cell are not equivalent [1]. An extensive density functional theory (DFT) calculation on the *25-on-23* unit cell now shows four hills with very similar heights. The corrugation of 120 pm is in line with a recent DFT calculation on a 11x11 super cell, assuming a 12×12 graphene on 11×11 Ru(0001) coincidence lattice [5]. However, the four hills do not have the same registry of their summit positions with respect to the graphene lattice. The theoretical prediction is one hill with a tetrahedral (Y) apex consisting of four carbon atoms, and three omega (Ω) peaks with carbon six-rings on the crest (see Fig. 14.2). In atomically resolved large scale scanning tunneling microscopy (STM) images it is possible to distinguish the two types of hills within the unit cell. When the structure taken from the DFT calculations is used to model the surface x-ray diffraction data, a better R-factor is obtained without adjustment of any parameters. Moreover, a lower graphene straining (Keating) energy results in comparison with the earlier structural model [6].

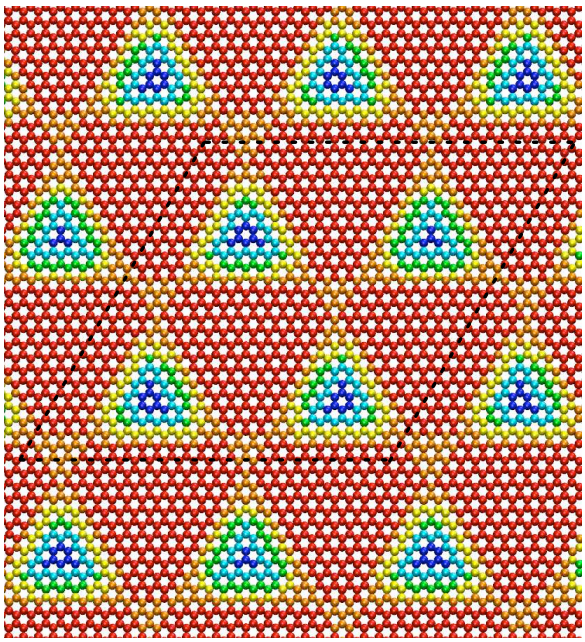

FIG. 14.2 – *Theoretical result for the arrangement of the 1250 carbon atoms in the 25-on-23 g/Ru(0001) structure (dashed parallelogram). The color indicates the height of the C atoms above the Ru substrate and ranges from 325 pm (blue) to 209 pm (red). Note the two different types of hills: one Y-type hill with one carbon atom on the apex and three Ω-type hills with six carbon atoms centered around the crest of the peak.*

[1] D. Martoccia, *et al.*, Phys. Rev. Lett. 101, 126102 (2008).

[2] T. Brugger, *et al.*, Phys. Rev. B 79, 045407 (2009).

[3] A. J. Pollard *et al.*, Angew. Chem. Int. Ed. 49, 1794 (2010).

[4] HG. Zhang *et al.*, J. Phys.: Condens. Matter 22, 302001 (2010).

[5] D. Stradi *et al.*, Phys. Rev. Lett. 106, 186102 (2011).

[6] D. Martoccia *et al.*, New J. Phys. 12, 04302 (2010).

14.2 Rashba effect in Pb quantum well states

In collaboration with: Gustav Bihlmayer, Peter Grünberg Institut and Institute for Advanced Simulation, Forschungszentrum Jülich and JARA, 52425 Jülich, Germany; Luc Patthey, Swiss Light Source, Paul Scherrer Insititute, 5232 Villigen.

When the thickness of a metal layer on a semiconductor is reduced to the coherence length of the conduction electrons, quantum confinement between the semiconductor band-gap and the image potential outside the metallic surface results in the formation of quantum well states (QWS) with quantized energy levels. These confined electrons, while bouncing back and forth between the metal-substrate and metal-vacuum interface, are free to move within the film plane, thus forming a prototypical two-dimensional electron gas (2DEG). The asymmetric confinement of the 2DEG results in the lifting of the spin degeneracy of the electronic states via the spin-orbit interaction (SOI), described by the Rashba effect [1]. The spin texture of a Rashba system consists of tangentially aligned spins of opposite direction on the spin split concentric Fermi circles centered around the $\overline{\Gamma}$ point, forming two spin vortices in momentum space.

This scenario was confirmed experimentally for QWS in ultrathin Pb films on Si(111) [2]. The study yielded two unexpected results: (i) the degree of spin splitting did not depend on the film thickness, and (ii) the helicity of the spin vortices was reversed when compared to the surface state on Au(111). Finding (i) suggested that the Rashba effect arises from contributions within the entire Pb layer rather than from the interfaces only. This is consistent with the understanding that the Rashba-type spin splitting is produced by the local asymmetry of the wave functions close to the Pb nuclei, where the Coulomb potential gradient is very strong [3]. In this model both, the metal-substrate and the metal-vacuum interfaces play a significant role by inducing an asymmetric wave function envelope due to the different penetration depths into the confinement barriers. To test this model we have grown ultra-thin Pb layers on different interfaces while keeping the metal-vacuum interface constant [4].

Figure 14.3(a) shows the measured momentum dependent spin splittings for samples where the Pb quantum films were grown on a preformed $\sqrt{3}\times\sqrt{3}$-R30° reconstructed surface induced by either Pb, Bi or Ag. Compared with the Pb interface, we find a reduction of the Rashba effect by almost 50 % on

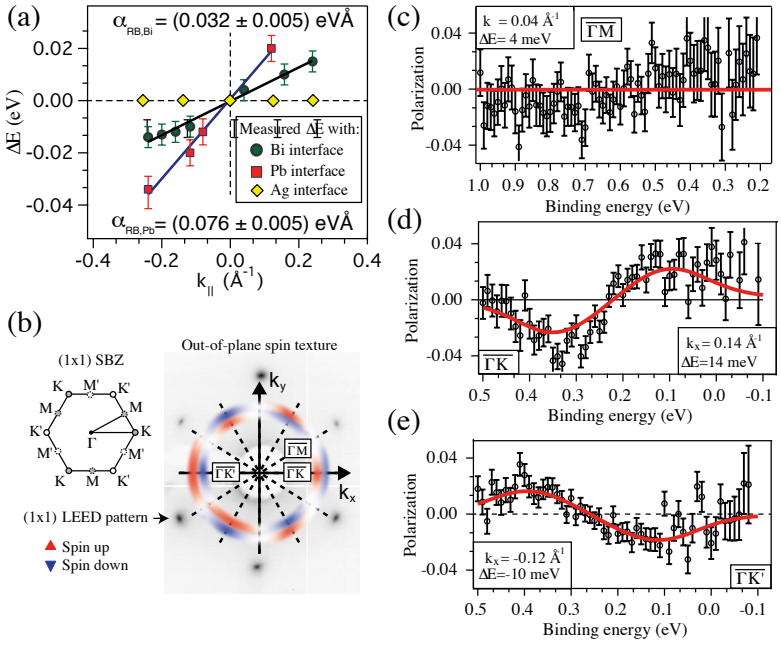

FIG. 14.3 –

(a) Measured spin splittings of Pb QWS for different interfaces between the Pb film and the Si(111) substrate, plotted at different in-plane momenta. The linear fit is used to obtain the Rashba parameter.

(b) Out-of-plane spin texture in Pb/Bi/Si(111).

(c-e) Spin polarization data of the z-component taken at different high symmetry directions [4]).

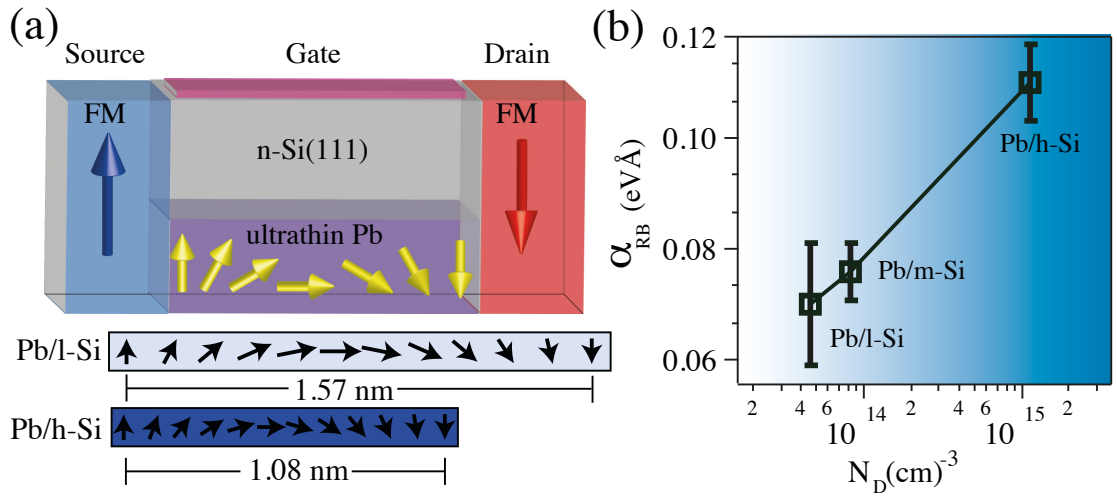

FIG. 14.4 – *(a) Schematic drawing of a spin-field-effect transistor with expected 180° spin rotation lengths in a lightly (Pb/l-Si(111)) and heavily (Pb/h-Si(111)) n-doped system. (b) shows the dependence of the experimentally determined Rashba parameters on the n-Si substrate doping.*

the Bi-reconstructed Si(111), while on the Ag interface the spin splitting drops below the resolution of our spin detector. It is concluded that the strength of the SOI can be manipulated through interface engineering, and that the Ag interface induces an almost symmetric charge distribution within the Pb film. Moreover, we have measured an out-of-plane spin polarization in the Pb/Bi/Si(111) system, which follows the three-fold symmetry of the lattice. This is seen in Fig. 14.3(b-e): along the $\overline{\Gamma}$-$\overline{M}$ direction of the (1x1) surface the spin polarization is fully in-plane, i.e. the z-polarization is zero, while it points out-of-plane along $\overline{\Gamma}$-$\overline{K}$. Since this system is non-magnetic, time-reversal symmetry dictates a reversal of the z-polarization along $\overline{\Gamma}$-$\overline{K'}$. This is exactly what we observe.

One of the main goals in the field of *spintronics* is the realization of a spin-based field-effect transistor [5] with the following operating principle (Fig. 14.4(a)): a Rashba system forms a 2D channel between ferromagnetic (FM) source and drain electrodes. Depending on whether the electron spins are aligned parallel or antiparallel with the magnetization direction of the drain after propagating along the channel, a high or low current passes through. The SOI permits to control the momentum splitting, and consequently the degree of spin rotation in the channel, by means of an externally applied gate voltage rather than through an external magnetic field. A large step towards the realization of such a device is our recent investigation of the dependence of the Rashba effect on the doping level of the n-type Si(111) substrate. As can be seen from Fig. 14.4(b) the strength of the SOI can be tuned effectively: a change in the donor concentration by a factor of ∼20 raises the Rashba constant by almost a factor of two. We conjecture that the gradient of the band bending at the film-substrate interface is the decisive factor for this effect. This finding opens up the possibility to tune the Rashba-type spin splitting in metallic QWS via an externally applied gate voltage.

[1] Y. A. Bychkov and E. I. Rashba, J. Phys. C: Solid State Physics, 17, 6039 (1984).

[2] J. H. Dil *et al.*, Phys. Rev. Lett. 101, 266802 (2008).

[3] G. Bihlmayer *et al.*, Surf. Sci., 600, 3888 (2006).

[4] B. Slomski *et al.*, Phys. Rev. B, 84, 193406 (2011).

[5] S. Datta and B. Das, Appl. Phys. Lett. 56, 665 (1990).

14.3 Electron dynamics in a quasi-one-dimensional topological metal: Bi(114)

A few years ago, a new class of materials called topological insulators was predicted and later on experimentally demonstrated [1], which exhibit spin-polarized and topologically protected surface states owing to strong spin-orbit interaction. More recently, a so-called topological metal was discovered on the Bi(114)-surface, which consists of atomic rows that support a one-dimensional surface state [2]. The Fermi line corresponding to the Fermi surface of the surface state is spin split as shown by spin-resolved photoelectron spectroscopy [2] and circular dichroism in the angular distribution [3].

We performed time-resolved photoelectron spectroscopy experiments on the Bi(114) surface. The electron-electron scattering rates are found to be extremely low due to the low density of states close to the Fermi level and due to the spin structure of the surface states, resulting in picosecond lifetimes. In contrast to the weak electron-electron scattering, electron-phonon interaction is quite strong in bismuth owing to its rhombohedral crystal structure, in which slight deviations from the simple cubic structure cause huge changes in the electronic density of states.

Surprisingly, the complex interplay of electronic and phonon degrees of freedom can be cast into a simple model involving three coupled rate equations for electrons, the bath of weakly coupled phonons, referred to as the *lattice*, and a subset of strongly coupled phonons, which dominates the response to the coherent excitation in a way very similar to the case of high-Tc superconductors [4]. The electronic temperature rise after excitation can be extracted from our spectra by fitting a Fermi-Dirac distribution or by evaluating the excess energy in the electron gas. The results of fitting the three differential equations to the electronic temperature data are shown in Fig. 14.5. The resulting coupling parameter indicates a strong coupling and a high occupation by several quanta of each single mode.

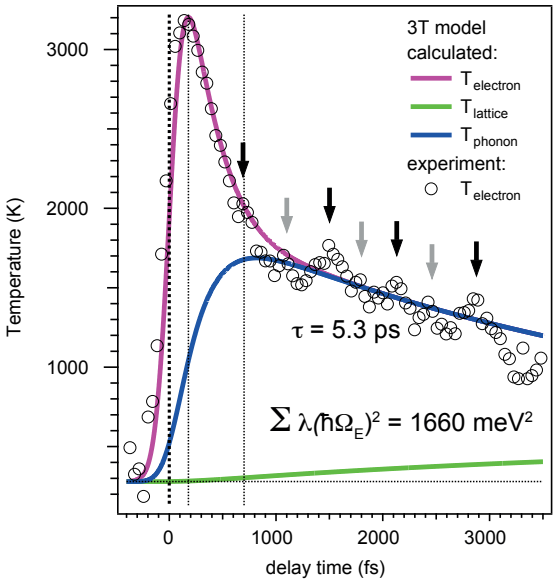

FIG. 14.5 – *Evolution of the electronic temperature after absorption of the laser (pump) pulse at time delay zero (open symbols). The rise and subsequent decay on two distinct timescales can be fitted by using different temperatures for electrons (purple line), for a subset of strongly coupled phonons (blue line), and for the general lattice (green line). The term* $\sum \lambda(\hbar\Omega_E)^2$ *indicates the coupling strength between electrons and the particular phonon subset summed over all modes. The arrows mark maxima in the electronic spectra, which are caused by excitation of coherent phonon modes. These oscillations were ignored in the three-temperature analysis.*

Moreover, the spectra of the hot electron gas exhibit energy and intensity oscillations due to the excitation of coherent phonon modes [5, 6], as shown in Fig. 14.6. The Fourier transforms of the transients can be used for identifying the involved phonon modes by comparing the frequencies with calculated phonon band structures for bismuth [7]. We deduce from our data that a transverse optical phonon mode with a frequency of 0.72 THz and a maximum density of states close to the X-point of the bulk Brillouin zone drives the observed intensity and binding energy oscillations of the electronic states at the Fermi level. Since the X-point corresponds to a standing wave along the direction of the atomic chains on Bi(114), the strong suscep-

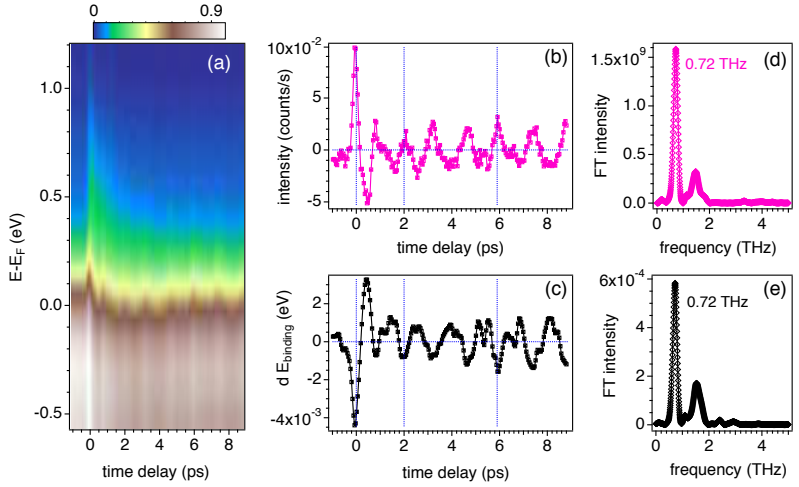

FIG. 14.6 – *(a) Time-resolved photoemission data on a false-color scale as function of delay and binding energy. Close to delay zero unoccupied states above the Fermi energy are populated; the excited states decay and show intensity and energy modulations. Center panels show the measured oscillations in intensity (b) and energy (c), and (d, e) the corresponding Fourier transforms.*

tibility of the quasi-one-dimensional electron gas in the chains to perturbations could explain why this particular phonon mode had never been observed so far in time-resolved experiments.

[1] D. Hsieh *et al.*, Science 323, 919 (2009).
[2] J. Wells *et al.*, Phys. Rev. Lett. 102, 096802 (2009).
[3] D. Leuenberger, Ph.D. thesis, University of Zurich (2011).
[4] L. Perfetti *et al.*, Phys. Rev. Lett. 99, 197001 (2007).
[5] M. Hase *et al.*, Phys. Rev. Lett., 88 (2002).
[6] D. Fritz *et al.*, Science, 315 (2007).
[7] E.D. Murray *et al.*, Phys. Rev. B 75, 184301 (2007).